Hindawi
Advances in Civil Engineering
Volume 2019, Article ID 1053576, 10 pages
https://doi.org/10.1155/2019/1053576

Research Article

Supporting Characteristics of Soldier Piles for Foundation Pits under Rainfall Infiltration

Changxi Huang[1], **Xinghua Wang**[1], **Min Zhang**[2], **Hao Zhou**[1] and **Yan Liang**[1]

[1]*School of Civil Engineering, Central South University, Changsha 410075, China*
[2]*School of Architecture and Civil Engineering, Taiyuan University of Technology, Taiyuan 030024, China*

Correspondence should be addressed to Xinghua Wang; xhwang@mail.csu.edu.cn

Received 14 November 2018; Accepted 12 June 2019; Published 26 June 2019

Academic Editor: Khalid Abdel-Rahman

The evolution of supporting characteristics of soldier piles for foundation pits under rainfall infiltration is described in this paper. Based on the Richards seepage equation and earth pressure theory considering the effect of intermediate principal stress of unsaturated soil, the approximate solution of permeability coefficient in unsaturated soil is developed using the Laplace integral transform and residue theorem. The transition of the boundary condition from flux boundary to head boundary is taken into account, and the rationality of the solution is verified. The safety factor of soldier piles' stability against overturning is derived, and its displacements are obtained by the finite-difference method. The results show that the stability of soldier piles gradually decreases with rainfall duration, and the actual embedded depth of the pile should be greater than the minimum embedded depth specified by the design code. The displacement response of pile top lags behind the rainfall and increases later in the rainfall period. The hysteresis time is shortened with the increase of soil permeability. Considering moisture absorption, the effect of rainfall on the properties of retaining structure is limited for the homogeneous soils with low suction or permeability.

1. Introduction

For foundation pit excavation in rainy areas, the most prominent problem is foundation pit instability caused by rainwater infiltration. In rainy season, rainfall increases the water content of shallow soil of foundation pits, which forms a transient saturation zone and expands downward; the change of pore water pressure in the soil will cause seepage and additional permeable pressure, which leads to the increase of soil sliding force or soil loss between piles. In addition, with the infiltration of rainwater, the contribution of the matric suction to the shear strength of soil decreases or even completely loses, which results in the decrease of resistance in the potential slip surface. As a result, the safety of the foundation pit declines.

Natural foundations are mostly unsaturated. There are capillary pressure phenomena and coupling effects between three phases which are soil particles, water, and gases in the unsaturated soil. Wu et al. [1] pointed out that the internal force of the retaining structure of the foundation pit significantly reduced considering the suction of unsaturated soil, which should be taken advantage of in design. Aqtash and Bandini [2] predicted the unsaturated shear strength of the adobe soil, which increases obviously with soil suction. Khaboushan et al. [3] studied the relation between soil characteristics and unsaturated shear strength parameters. The shear strength parameters can be predicted based on the soil properties. Moreover, Leong and Abuel-Naga [4] found that there is little effect of osmotic suction on the shear strength of unsaturated silt. However, matric suction affects the shear strength of unsaturated soil. Kim et al. [5] analyzed hysteresis effects on the mechanical property of unsaturated granite soil by the finite element method. It shows that the matric suction is small with the main wetting curve.

The establishment of the rainfall infiltration model of unsaturated soil and the determination of matric suction distribution at different times are the prerequisites for analysis of foundation pits or slopes under rainfall conditions. Wu and Huang [6] established one-dimensional transient and steady state models under rainfall infiltration

with the flux and pore pressure boundaries in unsaturated soils, taking into account the variation of rainfall intensity. Wu et al. [7] studied the seepage problem under the coupling effect of deformation and seepage. Oh and Lu [8] analyzed the transient slope stability under rainfall in a generalized effective stress framework, which increases three unsaturated parameters to the saturated conditions. The theory framework was used to reproduce the slope failure in practice. Dou et al. [9] obtained the failure probability of unsaturated slope over time with rainfall by the Monte Carlo method. Furthermore, Song et al. [10] investigated the unsaturated slope stability in real time according to the suction stress attained from monitoring data. Sun et al. [11] provided a three-phase model to simulate the dynamic change of safety factor with a given slip surface of unsaturated slope under rainfall infiltration. Cho [12] studied the influence of pore-air pressure variation on the slope stability due to rainfall. A numerical study shows that air flow contributes to the silt slope stability but air flow is adverse to the stability of sandy slope. In addition, other scholars carried out relevant studies on two-dimensional rainfall infiltration [13] and double-layer foundation [14].

From the literature review, the research on the unsaturated soil stability under rainfall infiltration mainly focused on slopes or landslides [14–16] and less on foundation pits. Although they had similarities in stability checking, the foundation pits were different from slopes in support form, instability mechanism, and analysis methods. At present, there is lack of comprehensive quantitative study on the evolution law of stability and deformation characteristics of supporting structures of foundation pits with rainfall, which is a worthy theoretical and engineering subject.

In this paper, based on the Laplace integral transformation and finite-difference method, approximate solution of permeability coefficient in unsaturated soil during rainfall infiltration is obtained considering the boundary transition from flux boundary to head boundary. A theoretical model for calculating the stability and deformation characteristics of soldier piles of foundation pit is established. The rainfall infiltration effect on the supporting structure of foundation pit is discussed through parameter analysis.

2. Calculation Model and Unsaturated Soil Pressure

Figure 1 is the calculation model of soldier piles of foundation pit under rainfall. The coordinate origin is located on the soil surface; z axis positive direction points to the soil vertically. The excavation depth of foundation pit is H, embedded depth is D, and pile length is $L = H + D$. The groundwater level in active and passive earth pressure areas are L_a and L_p, respectively. q_A is the initial steady flow into the soil surface; q_B is the rainfall intensity.

In order to simplify the calculation, the assumptions are introduced as follows: (1) the soil is a homogeneous isotropic unsaturated medium, and soil surface is a permeable boundary; (2) supporting piles are equal in diameter, regardless of their friction and spatial effects; (3) rainfall intensity is constant, neglecting the seepage effect caused by the groundwater level difference between the active and passive zones; (4) the bottom of the foundation pit and the soil behind the pile are at the Rankine limit stress state. In addition, the purpose of this paper is to study the influence of matric suction on shear strength and earth pressure of soil, without considering the soil stiffness weakening caused by long-term immersion or periodic soaking-air drying under natural environment.

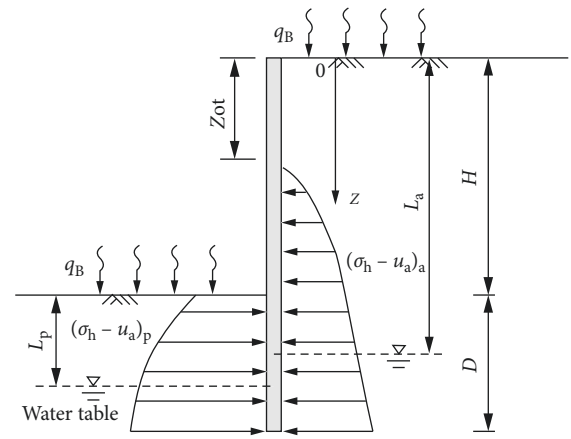

Figure 1: Computation model for deep excavation under rainfall.

According to [17], the shear strength of unsaturated soils can be obtained on the basis of unified strength theory and Bishop effective stress principle.

$$\tau_f' = c_t' + [(\sigma - u_a) + \chi(u_a - u_w)]\tan\varphi_t', \quad (1)$$

where σ is the total normal stress, τ_f' is the effective shear strength, and χ is the effective stress coefficient of unsaturated soil. u_a and u_w are the air pressure and water pressure, respectively; $u_a - u_w$ is the matric suction. c_t' and φ_t' are the unified effective cohesion and unified effective internal friction angle, respectively which can be calculated by $c_t' = (2(1+b)c'\cos\varphi')/2 + b(1+\sin\varphi')(1/\cos\varphi_t')$ and $\sin\varphi_t' = (2(1+b)\sin\varphi'/2 + b(1+\sin\varphi'))$. c' and φ' are the effective cohesion and effective internal friction of soil, respectively. b is the unified strength theory parameter which reflects the influence of intermediate principal stress on the yield or failure of materials. The range of value is $0 \le b \le 1$.

There is a highly nonlinear relationship between χ and matric suction or saturation. The range of χ is from 0 to 1, which reflects the contribution of suction stress to soil shear strength. It also shows that there is a nonlinear functional relationship between unsaturated soil shear strength and matric suction. Based on equation (1), unsaturated Rankine active and passive earth pressure can be obtained, which considers intermediate principal stress as follows [18]:

$$\sigma_h - u_a = (\sigma_v - u_a)k_a - 2c_t'\sqrt{k_a} - \chi(u_a - u_w)(1 - k_a), \quad (2a)$$

$$\sigma_h - u_a = (\sigma_v - u_a)k_p + 2c_t'\sqrt{k_p} + \chi(u_a - u_w)(k_p - 1), \quad (2b)$$

where σ_h and σ_v are the horizontal and vertical stresses, respectively. $k_a = \tan^2((45 - \varphi_t')/2)$ is the active earth pressure coefficient; and $k_p = \tan^2((45 + \varphi_t')/2)$ is the passive earth pressure coefficient.

Equations (1) and (2) indicate that soil shear strength reduces with the decrease of matric suction. Rainfall infiltration increases the degree of saturation, which leads to a disadvantageous situation. The earth pressure can be calculated according to limit stress state. In addition, the matric suction is nonlinear along the depth direction in practice, especially under the effect of water infiltration and moisture absorption. It means that the distribution of lateral earth pressure has complex space-time characteristics under rainfall conditions.

3. Model Solution

3.1. Rainfall Intensity Is Less than Saturated Permeability Coefficient. For homogeneous isotropic soils, the permeability coefficient and soil-water characteristic curve of unsaturated soils can be described by the exponential function proposed by Gardner [19]:

$$k(h_m) = k_s \exp(\beta h_m), \tag{3a}$$

$$\frac{\theta - \theta_r}{\theta_s - \theta_r} = \exp(\beta h_m), \tag{3b}$$

where h_m is the suction head, which is calculated by $h_m = (-(u_a - u_w)/\gamma_w)$; γ_w is the unit weight of water; k is the unsaturated permeability coefficient related to matric suction; k_s is the saturated permeability coefficient; θ is the volume water content of soil; θ_s and θ_r are the saturated and residual water content, respectively; and β is the decreasing rate of permeability coefficient with the increase of suction. It ranges from 0 to 5 per meter. For coarse grained soil, β can have large values, while for clay and silt, it would be small.

Combined with boundary and initial conditions, Srivastava and Yeh [20] derived the permeability coefficient between the ground surface and groundwater level by the Laplace transform on the one-dimensional transient unsaturated Richards seepage equation and inverse transformation based on residue theorem.

$$K_1(Z,T) = Q_B - \left(Q_B - e^{-\beta h_0}\right)e^{-(\overline{L}_a - Z)} - 4(Q_B - Q_A)e^{Z/2}e^{-T/4} \cdot \sum_{n=1}^{+\infty} \frac{\sin[\lambda_n(\overline{L}_a - Z)]\sin(\lambda_n \overline{L}_a)e^{-\lambda_n^2 T}}{1 + \left(\overline{L}_a/2 + 2\lambda_n^2 \overline{L}_a\right)}, \tag{4}$$

where λ_n is the n th root of the following equation:

$$\tan(\lambda \overline{L}_a) + 2\lambda = 0, \tag{5}$$

where $Z = \beta \cdot z$; $K = k/k_s$; $Q_A = q_A/k_s$; $Q_B = q_B/k_s$; $T = (\beta \cdot k_s \cdot t)/(\theta_s - \theta_r)$; $\overline{L}_a = \beta L_a$; z is the soil depth; and t the is rainfall duration. h_0 is the suction head at groundwater level, and it is usually assumed to be zero.

3.2. Rainfall Intensity Is Greater than Saturated Permeability Coefficient. When rainfall intensity is greater than the saturated permeability coefficient, ponding or runoff occurs on the ground surface and pit bottom after a period of rainfall. It means that there is a totally saturated state. When suction head decreases to zero, the time (T_0 or t_0) when it begins to saturate at ground surface can be calculated from equation (4). Fourier integral transformation was used to solve the problem in [21]. However, the initial condition in this paper is different from equation (4). Therefore, Laplace integral transformation is used to deduce the approximate solutions of the permeability coefficient.

When rainfall duration (t) is less than t_0, the rainwater infiltrates completely. There is no rainwater accumulation on the ground surface and foundation pit bottom. The upper boundary is still the flux boundary condition:

$$\left[-\frac{\partial K}{\partial Z} + K\right]_{Z=0} = Q_B. \tag{6}$$

At this stage, the permeability coefficient can be obtained by equation (4). When t is greater than t_0, rainwater accumulates on the ground surface and at the bottom of the pit. Therefore, soil suction disappears. The upper boundary changes into head boundary as follows:

$$K_2|_{Z=0} = 1. \tag{7}$$

At this time, the law of rainfall infiltration is not affected by rainfall intensity any more. It only plays the role of head boundary. Combining with boundary condition equation (6), permeability coefficient in unsaturated region is obtained by Laplace integral transformation of time T in Richards equation in [18].

$$\overline{K}_2(Z,s) = \frac{Q_A - (Q_A - e^{-\beta h_0})e^{-(\overline{L}_a - Z)}}{s} + \left[1 - Q_A + \left(Q_A - e^{-\beta h_0}\right)e^{-\overline{L}_a}\right]e^{Z/2} \cdot F(s), \tag{8}$$

where $F(s)$ is calculated by $F(s) = (1/s)((\sinh(\sqrt{s + (1/4)}\,(\overline{L}_a - Z)))/(\sinh(\sqrt{s + (1/4)}\,\overline{L}_a))) = p(s)/q(s)$ and s is the Laplace transform coefficient. It should be noted that the second term on the left side of the original formula should be changed to minus in calculation since the z axis positive direction (downward) of the model in this paper is exactly opposite to that of Richards governing equation (5) in reference [20].

Using the residue theorem, the result of Laplace inverse transformation of $F(s)$ is as follows:

$$F(T) = \sum_{k=1}^{n} \mathrm{Res}\left[F(s)e^{sT}, s_k\right] = \sum_{k=1}^{n} \frac{p(s_k)}{q'(s_k)}, \tag{9}$$

where $q'(s)$ represents the first derivative of $q(s)$ and s_k is the k th isolated singularity.

According to the above theorem, the inverse transformation expression of $F(s)$ can be obtained.

$$F(T) = \frac{\sinh[(\overline{L}_a - Z)/2]}{\sinh(\overline{L}_a/2)} + \sum_{n=0}^{+\infty} \frac{(-1)^n 8\pi n \cdot \sin(\pi n(\overline{L}_a - Z)/\overline{L}_a)}{\left(4\pi^2 n^2 + \overline{L}_a^2\right)} e^{-\left(\left(\pi^2 n^2/\overline{L}_a^2\right)+(1/4)\right)T}. \tag{10}$$

The first term on the right-hand side of the equation is the residue as s equals zero. The summation terms correspond to residues at the isolated singular point $\sqrt{s_n + (1/4)}\,\overline{L}_a = in\pi$ in the complex field.

Putting equation (10) into equation (8), the permeability coefficient at any time and depth can be obtained for the second stage ($t \geq t_0$).

$$K_2(Z,T) = Q_A - \left(Q_A - e^{-\beta h_0}\right)e^{-(\overline{L}_a - Z)} + \left[1 - Q_A + \left(Q_A - e^{-\beta h_0}\right)e^{-\overline{L}_a}\right]e^{Z/2} \cdot F(T). \tag{11}$$

It is worth noting that the initial condition is $t < t_0$ during the above derivation.

$$K(Z,0) = Q_A - \left(Q_A - e^{-\beta h_0}\right)e^{-(\overline{L}_a - Z)} = K_0(Z). \tag{12}$$

The initial condition of $t > t_0$ can be attained by equation (4) with $T = T_0$. However, it is difficult to get the exact expression of permeability coefficient because of the complexity of equation (4). Equation (11) is only an approximate solution expression. The result of trial calculation shows that the distribution of K_1 and K_2 are approximately same at T_0. K_2 is generally larger than K_1 except for ground surface and groundwater level where both K_2 and K_1 equal one. K_2 tends to be 1.0 while T is close to infinity. Therefore, K_2 is modified on the basis of the linear proportional distribution of the difference between K_2 and K_1 at T_0. The result is as follows:

$$\overline{K}_2(Z,T) = K_2(Z,T) - \Delta_0(Z)\frac{1 - K_2(Z,T)}{1 - K_2(Z,T_0)}. \tag{13}$$

The above deductions are all aimed at the solution of the permeability coefficient in the active zone while the solution in the passive zone can be attained by replacing L_a with L_p.

3.3. Finite-Difference Solution of Permeability Coefficient. In order to verify the rationality and accuracy of the approximate solution in Section 3.2, permeability coefficient in the second stage of rainfall is calculated by finite-difference method under the actual initial conditions (permeability coefficient is K_1 at the time of T_0). The unsaturated soil region is discretized by space and time. The depth of the soil is divided into n equal segments. The time step and space step are recorded as ΔT and ΔZ, which are dimensionless. When the time step is very small, the Richards' percolation equation in [18] can be discretized into the following differential form:

$$aK_{i,j-1} + bK_{i,j} + cK_{i,j+1} = dK_{i-1,j}, \tag{14}$$

where $a = \Delta T \times (1 + \Delta Z)$; $b = -\Delta Z \times \Delta T - 2 \times \Delta T - \Delta Z \times \Delta Z$; and $c = \Delta T$; $d = -\Delta Z \times \Delta Z$. i and j represent time and space nodes, respectively. $i = 1, 2, \ldots$; $j = 1, 2, \ldots, n+1$. $T_{i=1} = 0$ represents the time T_0 (or t_0) that rainwater begins to accumulate on the ground surface. $Z_{j=1} = 0$; $Z_{j=n+1} = \overline{L}_a$. $K_{i,j}$ is the dimensionless permeability coefficient with $T_i = i \times \Delta T$ and $Z_j = j \times \Delta Z$. The corresponding boundary conditions can be discretized into the following equation:

$$\begin{aligned} K_{i,1} &= 1, \\ K_{i,n+1} &= 1. \end{aligned} \tag{15a}$$

After putting $T = T_0$ into equation (4), the permeability coefficient is taken as the initial condition of the second stage. The discrete form is as follows:

$$K_{1,j} = K_1\left(Z_j, T_0\right). \tag{15b}$$

It is clear that the difference form for the flux boundary condition in the first stage of rainfall is as follows:

$$K_{i,1} = \frac{K_{i,2} + \Delta Z \times Q_B}{1 + \Delta Z}. \tag{16}$$

Different differential equations are set up for each node in the differential grid, respectively.

$$\begin{pmatrix} b & c & 0 & 0 & \cdots & 0 \\ a & b & c & 0 & \cdots & 0 \\ \vdots & \vdots & \vdots & \vdots & \vdots & \vdots \\ 0 & \cdots & a & b & c & 0 \\ 0 & \cdots & 0 & a & b & c \\ 0 & 0 & \cdots & 0 & a & b \end{pmatrix}_{(n-1)\times(n-1)} \begin{pmatrix} K_{i,2} \\ K_{i,3} \\ \vdots \\ K_{i,n-1} \\ K_{i,n} \end{pmatrix} = \begin{pmatrix} dK_{i-1,2} - aK_{i,1} \\ dK_{i-1,3} \\ \vdots \\ dK_{i-1,n-1} \\ dK_{i-1,n} - cK_{i,n+1} \end{pmatrix}. \tag{17}$$

Accordingly, the Richards seepage equation is transformed into algebraic equations.

It can be seen that equation (17) is a set of linear equations about the unknown numbers of $K_{i,j}$. The coefficient matrix is a strictly diagonally dominant triangular matrix, which can be solved recursively by the pursuit method.

3.4. Stability and Deformation of Embedded Soldier Piles. On the basis of the permeability coefficients of active and passive zones, suction head and effective stress coefficients can be obtained by equations (3a) and (3b). By bringing them into equations (2a) and (2b), the distribution of active and passive earth pressures of unsaturated soils can be obtained finally at any time and depth. When effective stress coefficient χ is expressed by a general van Genuchten model [22], equations (2a) and (2b) can be written as follows:

$$(\sigma_h - u_a)_a = \gamma z k_a - 2c_t' \sqrt{k_a} - \frac{(u_a - u_w)(1 - k_a)}{\left[1 + (a_0 (u_a - u_w))^{d_0}\right]^{1-(1/d_0)}}, \tag{18a}$$

$$(\sigma_h - u_a)_p = \gamma z k_p + 2c_t' \sqrt{k_p} + \frac{(u_a - u_w)(k_p - 1)}{\left[1 + (a_0 (u_a - u_w))^{d_0}\right]^{1-(1/d_0)}}, \tag{18b}$$

where a_0 and d_0 are the fitting parameters of V-G model and $(u_a - u_w) = -\gamma_w In[K(Z,T)]/\beta$. The subscripts a and p represent the active and passive limit state of soil respectively. γ is unit weight of soil above groundwater.

By substituting equations (4) or (13) into equation (18a), the critical depth z_{ot} can be obtained as active earth pressure $(\sigma_h - u_a)_a$ equals zero. Because the solution of transcendental equation is involved, numerical calculation methods such as Newton iteration can be used.

The safety factor of supporting piles stability against overturning can be expressed by the ratio of the resistance moment M_p formed by passive earth pressure around the pile bottom to the overturning moment M_a formed by active earth pressure. Both include the moments generated by unsaturated soils and effective unit weight and hydrostatic pressure of saturated soils. Therefore, the safety factor of piles stability against overturning can be expressed as

$$K_q = \frac{M_p}{M_a} = \frac{M_{pun} + M_{psa}}{M_{aun} + M_{asa}}, \tag{19}$$

where

$$M_{aun} = \int_{z_{ot}}^{L_a} (\sigma_h - u_a)_a (L - z) dz,$$

$$M_{asa} = \frac{\gamma_w (L - L_a)^3}{6} + (L - L_a)^2 \left\{ \frac{k_a [3\gamma L_a + \gamma' (L - L_a)]}{6 - c_t' \sqrt{k_a}} \right\},$$

$$M_{pun} = \int_0^{L_p} (\sigma_h - u_a)_p (D - z) dz,$$

$$M_{psa} = \frac{\gamma_w (D - L_p)^3}{6} + (D - L_p)^2 \left\{ \frac{k_p [3\gamma L_p + \gamma' (D - L_p)]}{6 + c_t' \sqrt{k_p}} \right\},$$

$$\gamma' = \gamma_{sat} - \gamma_w, \tag{20}$$

where γ' is the effective unit weight of the soil and γ_{sat} is the saturated unit weight of the soil.

For calculation of horizontal displacement of supporting piles, pile section above the excavation surface can be regarded as the cantilever section with embedded bottom. Pile section below the excavation surface can be taken as elastic foundation beam. So the deflection of each section can be calculated separately. The actual active earth pressure calculated during the rainfall process is considered as lateral load of the cantilever section while the load of anchorage section is rectangular load. The elastic deflection differential equation of soldier piles is as follows:

$$EI \frac{d y^4}{d^4 z} + b_0 K(z) y - b_0 p_a(z) = 0, \tag{21}$$

where y is the horizontal displacement; $p_a(z)$ is the distributed load acting on the supporting pile; EI is the flexural rigidity of the pile; and b_0 is the calculation spacing of the piles. $K(z)$ is the horizontal resistance coefficient of the foundation. Above the excavation surface, $K(z)$ equals zero while $K(z)$ equals mz below the excavation surface. m is the proportion coefficient of the foundation, which can be achieved by the relevant tables.

For elastic foundation beam, the bending moment and shear force at pile end are 0. ($EI \cdot y'' = 0$; $EI \cdot y''' = 0$). Equation (21) can be solved directly by the bvp5c function embedded in MATLAB software. For the cantilever section above the excavation face, it is difficult to solve equation (21) directly considering the nonlinear distribution of earth pressure. The cantilever section is discretized into N segments with a same length of Δh; $\Delta h = H/N$. The number of the nodes are 0, 1, 2, . . ., N. The displacement and rotation angle of the fixed end are zero ($y_N = 0$; $y_N' = 0$). Considering $y'' = M(z)/EI$, the displacement of the bottom node satisfies the following relationship:

$$\frac{y_{N+1} - y_{N-1}}{2\Delta h} = 0, \tag{22a}$$

$$y_{N+1} - 2y_N + y_{N-1} = \frac{(\Delta h)^2 M_N}{EI}, \tag{22b}$$

where y_{N+1} is the horizontal displacement of the virtual node $N + 1$ and M_N is the bending moment at the fixed end, which can be attained from the earth pressure above the excavation face.

According to equations (22a) and (22b), $y_{N-1} = (\Delta h)^2 \cdot M_N/(2EI)$ can be obtained. The displacements of other nodes can be calculated by the deduced difference form in [23]. The final displacement distribution of the pile body can be obtained by accumulating the translation and rotation displacement of the vertex of the embedded segment. Furthermore, internal force distribution of the pile body can be obtained.

4. Results and Discussion

A foundation pit is supported by bored piles with a diameter of 1.0 m, length of 10 m, and spacing of 1.4 m. The elastic modulus of concrete is 30 GPa. The depth of excavation is 6 m ($H = 6$ m), and embedded depth of pile is 4 m ($D = 4$ m). The depth of water table in active and passive earth pressure areas is 8 m and 2 m, respectively ($L_a = 8$ m; $L_p = 2$ m). The stratum is mainly silt. The unit weight γ of soil above the groundwater level is 18 kN·m^{-3}; the saturated unit weight γ_{sat} is 20 kN·m^{-3}. The saturated permeability coefficient k_s is 1.0×10^{-6} m/s; $\theta_s = 0.4$, $\theta_r = 0.15$, and $\beta = 0.5$ m^{-1}. The proportion coefficient of foundation m is 10 MN·m^{-4}; the unified strength theoretical parameter b is

0.5. In order to simplify the calculation, the effective cohesion c' and effective internal friction angle φ' of the soils are 10 kPa and 20°, respectively. The parameters of van Genuchten model a_0 and d_0 are 0.05 and 2, respectively. Initial steady flow q_A is $0\,m\cdot s^{-1}$; rainfall intensity q_B is $2.315\times10^{-6}\,m\cdot s^{-1}$ (equivalent to $200\,mm\cdot d^{-1}$).

Figures 2(a) and 2(b) are the distributions of suction head along depth when rainfall intensity is less and greater than saturated permeability coefficient, respectively. It can be seen that suction head has a linear distribution along the depth direction at the initial time. The suction at the groundwater level is 0. When rainfall begins, suction head near the ground surface decreases rapidly (absolute value). The suction reduction area gradually expands to the groundwater level with rainfall. Meanwhile, the wetting front advances downward. In the early stage of infiltration, rainfall mainly affects the suction in the upper part of the wetting front. From Figure 2(a), rainwater infiltrates into the soil completely. So, the suction head at the ground surface cannot be 0. In Figure 2(b), the permeability of the soil is too small, and thus rainwater cannot infiltrate totally. Hence, the ground surface is saturated with the water accumulation or runoff on the ground surface. As a result, suction head at the ground surface can be 0 as shown in Figure 2(b). In addition, the suction head calculated by the analytical method and the finite-difference method are basically in agreement, which verifies the rationality of the approximate solution. It provides a guarantee for the subsequent calculation of earth pressure.

Figure 3 shows that the relationship between safety factor against overturning and time under different rainfall intensities. The safety factor gradually decreases with the continuous rainfall. The safety factor declines obviously with greater rainfall intensity. With rainwater infiltration, degree of saturation gradually increases and matric suction of the soil decreases. Therefore, active earth pressure increases while passive earth pressure decreases, which leads to the increase of overturning moment acting on the supporting pile and decrease of resistance moment. Consequently, the safety factor decreases.

Figure 4 displays that the relation between safety factor against overturning and time under different saturated seepage coefficients. The selected permeability coefficient is less than rainfall intensity. The safety factor has a significant decline with the increase of permeability coefficient and rainfall duration. It is pointed out that supporting of foundation pit in a highly permeable foundation should cause attention. The increase of rainfall infiltration rate quickens up the downward expansion rate of the saturated region, which accelerates the reduction of the matric suction. It should be noted that the influence of rainfall infiltration on the foundation pit involves many factors, including soil moisture absorption, groundwater seepage, and water weakening. Reduction of suction, additional seepage force, and stiffness degradation of soil will reduce the safety of the foundation pit. In this paper, only the soil moisture absorption is analyzed, considering the complexity of the problem. Hence, the actual safety factor of piles stability against overturning should be lower than the result in Figure (4).

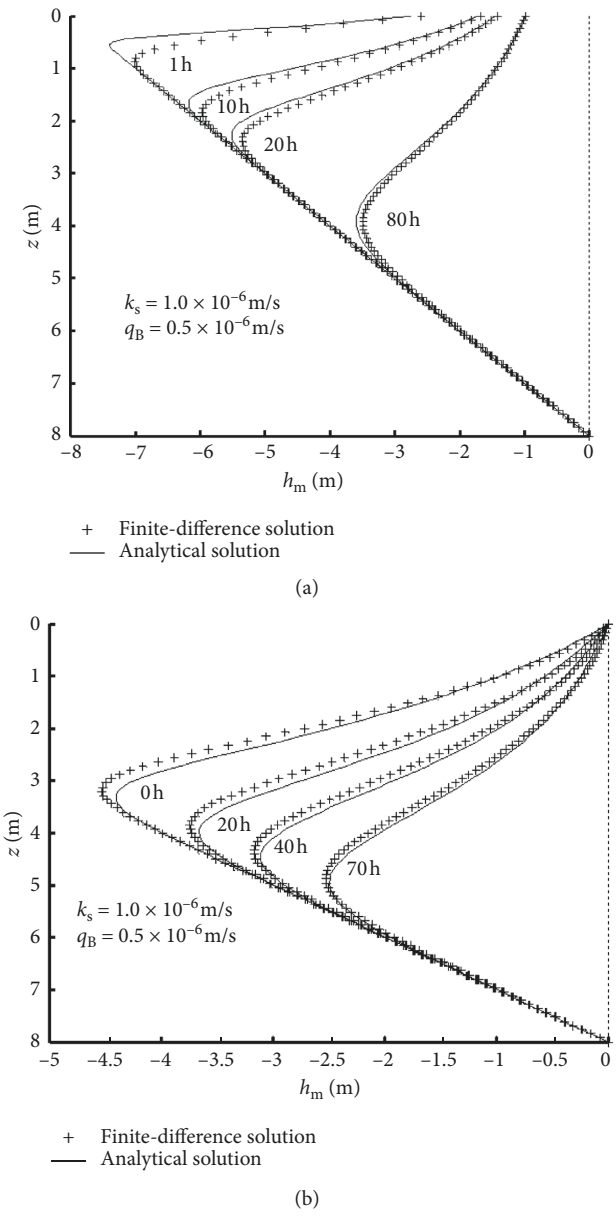

Figure 2: Distribution of suction head with depth at different time. (a) $q_B < k_s$. (b) $q_B > k_s$.

The influence of groundwater level depth on the safety factor against overturning is shown in Figures 5(a) and 5(b). Figure 5(a) shows that the groundwater level is the same on both sides of active and passive earth pressure zones, while Figure 5(b) illustrates that the groundwater level is different on both sides of active and passive earth pressure areas. It can be seen that the safety of foundation pit is gradually improved with the decrease of the groundwater level. It indicates that the less the groundwater level is, the better the stability of soldier piles will be. The reason is that the decrease of the water level increases the initial distribution range and amplitude of the suction. The suction contribution to soil shear strength is also fortified. Meanwhile, the active earth pressure decreases and the passive earth pressure increases, which improve the properties of retaining

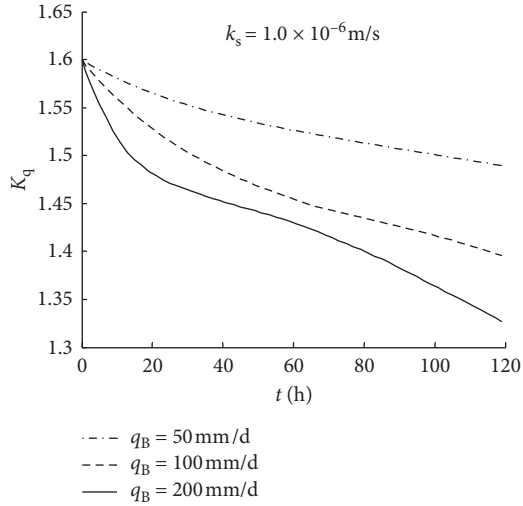

Figure 3: Effect of rainfall intensity on safety coefficient.

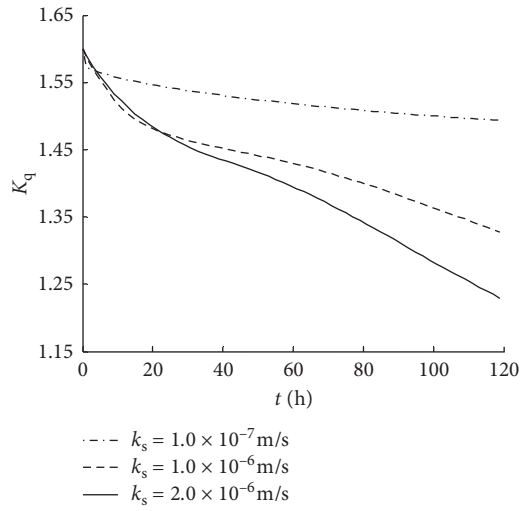

Figure 4: Effect of saturated permeability coefficient on safety coefficient.

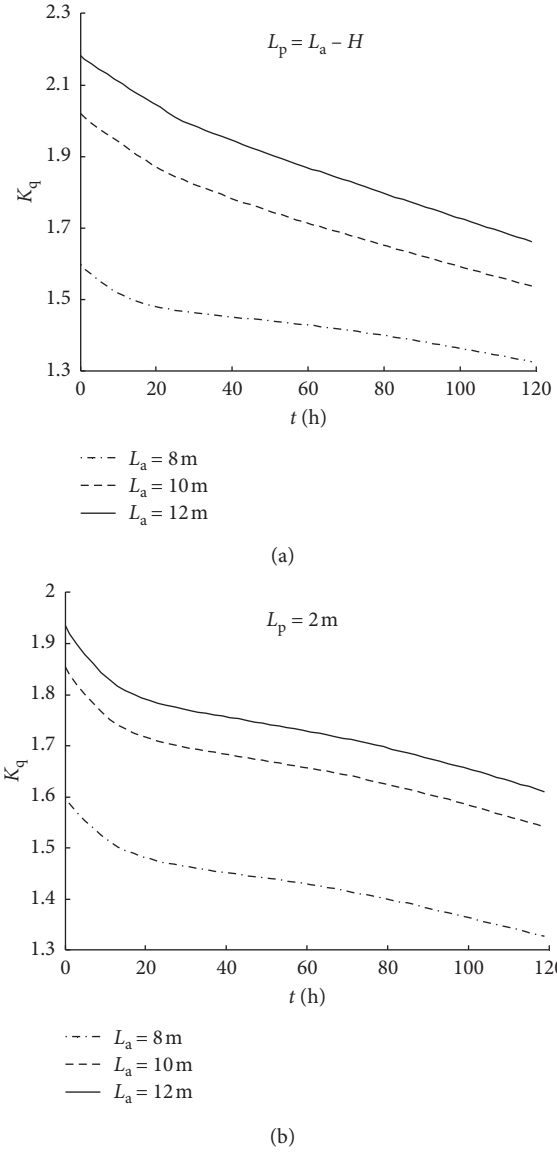

Figure 5: Effect of water table of active area on safety coefficient. (a) The same water table on both sides. (b) The different water table on both sides.

piles of foundation pit. In addition, decreasing the groundwater level on both sides of the active and passive zone at the same time improves the safety factor more obviously, compared with the one-sided decrease of groundwater level in the active zone. However, the safety factor of former decreases sharply as the time elapses.

Figures 6(a) and 6(b) describe the variation of safety factor against overturning with embedded depth and time as the unified strength theoretical parameter b is 0.0 or 1.0, respectively. It can be seen that the stability of foundation pit will be greatly improved with the increase of embedded depth. In Figure 6(a), the foundation pit may change from safe state to unstable state with the increase of rainfall duration as embedded depth is not large (f). This shows that the minimum embedded depth determined by the stability checking calculation in the foundation pit code should retain enough safety reserves to prevent adverse effects of rainfall from the stability of foundation pits. Parameter b reflects the effect of medium principal stress σ_2 on soil strength and failure; it also represents different strength criteria. Comparing Figures 6(a) and 6(b), it can be seen that the curve shape of the safety factor are basically the same under two b values. The safety factor at $b = 1$ is nearly 50%–80% higher than that at $b = 0$. It means that the design of supporting structure based on Mohr–Coulomb strength criterion is conservative. It is necessary to consider the effect of intermediate principal stress to achieve better economic benefits.

Figures 7 and 8 show the relationship between horizontal displacement of pile top and time under different rainfall intensities and saturated permeability coefficient, respectively. $a_0 = 0.01$ and $a_0 = 0.1$ represent silt and sand, respectively. From Figure 7, it can be seen that there is a lag for the displacement response as the time elapses. The

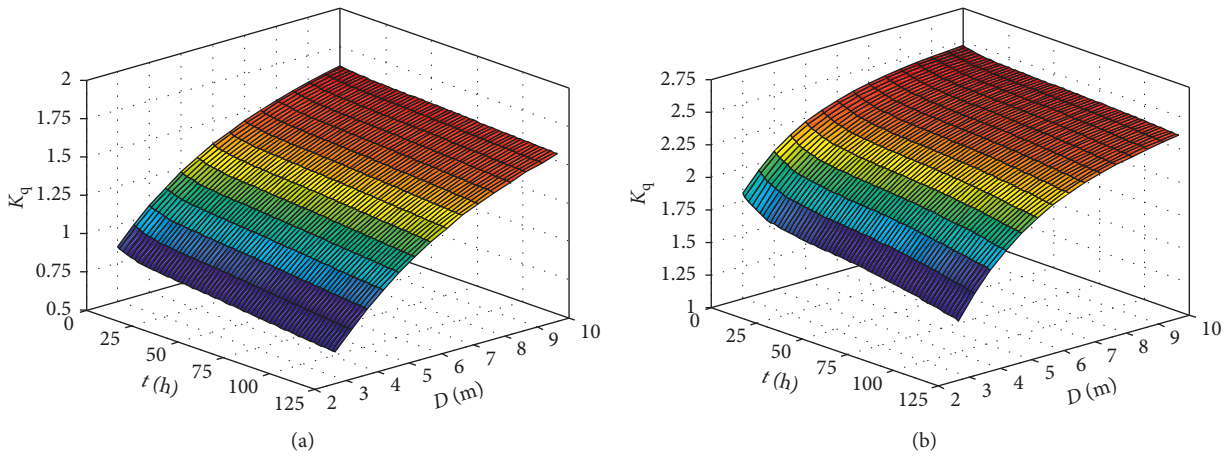

Figure 6: Variation of safety factor against overturning with embedded depth and time. (a) $b = 0.0$. (b) $b = 1.0$.

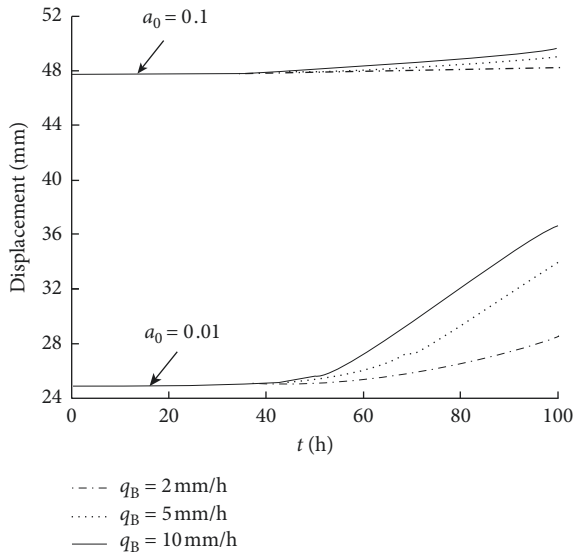

Figure 7: Effect of rainfall intensity on horizontal displacement of pile top.

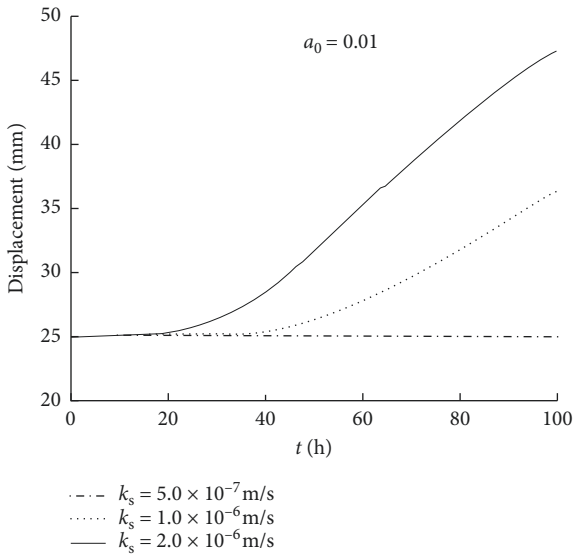

Figure 8: Effect of saturated permeability coefficient on horizontal displacement of pile top.

displacement of pile top is basically constant in the first half of the rainfall period. However, the displacement of pile top increases gradually later in the rainfall period. The lag time mainly depends on the permeability of the soil itself and is little affected by the rainfall intensity. The reason for displacement response hysteresis is shown as follows. Rainwater needs to go through the critical depth area where active earth pressure equals zero; then, it enters the area where the active earth pressure works. For silt or clay with high suction stress, critical depth can be several meters deep (about 4m in this case). Furthermore, the displacement of pile top in silt foundation increases significantly, especially in the case of heavy rainfall. However, for sandy soil foundation with low suction stress, the change of soil pressure caused by rainfall is limited. Thus, the displacement of pile top remains constant with time under different rainfall intensity. The maximum increase of displacement of pile top is only about 2mm . From Figure 8, it can be seen that the increase of saturated permeability coefficient k_s leads to a significant increase in the displacement of pile top, and a great decrease of the time that displacement response begins. The displacement of pile top at the end of rainfall almost doubles that at the beginning of rainfall while the saturated permeability coefficient is 2.0×10^{-6} m·s^{-1}, but the displacement of pile top remains constant as the saturated permeability coefficient is small.

In general, the characteristic of supporting structure is not very sensitive to short-term rainfall, especially for low permeability soil. Rainfall only affects the distribution of suction stress in the soil surface layer. However, for continuous rainy weather (such as $q_B = 2$ mm·h^{-1}), it is found that the displacement of pile top is 47 mm after 14 days, which should cause attention. Moreover, for expansive soils or soft soils, there may be more tension cracks in foundation pit wall under the condition of wet-dry cycling or excessive deformation of foundation pit. The cracks provide a rapid

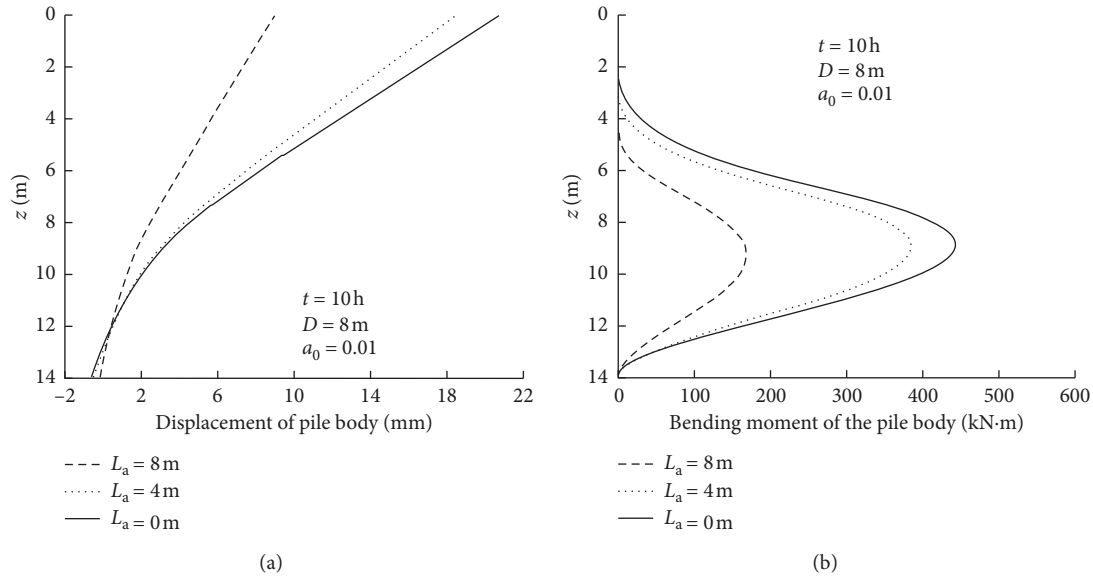

Figure 9: Effects of water table of active area on horizontal displacement and bending moment of pile. (a) Horizontal displacement of pile body. (b) Bending moment of pile body.

migration channel for rainwater infiltration into deep soils. Consequently, the permeability of surface soils will increase significantly. It is found that the wetting front arrives at critical depth within 1.5 hours when saturated permeability coefficient is $5 \times 10^{-5}\,\mathrm{m \cdot s^{-1}}$ and rainfall intensity is $30\,\mathrm{mm \cdot h^{-1}}$. The existence of soil cracks on the foundation pit wall greatly shortens the time of water infiltration into deep soil, which is extremely unfavorable to the stability of foundation pit.

When the embedding depth of soldier piles is 8m and rainfall duration is 10 hours, the distribution of displacement and bending moment of pile body are shown in Figure 9, considering three groundwater levels in active areas. It can be seen that the displacement and bending moment of pile body increase gradually with the decrease of water table; the critical depth of earth pressure moves up accordingly. The displacement of pile top for $L_a = 0$ m almost doubles that for $L_a = 8$ m. Compared to $L_a = 8$ m, the maximum bending moment of the pile increases by nearly 1.5 times for $L_a = 0$ m. However, the locations of the maximum bending moment on both water tables are 0.37 D below the excavation surface. Compared with the rise of shallow groundwater level, the rise of deep groundwater level has a more significant effect on the properties of soldier piles. This is because the soil suction stress is small under the high groundwater level and the critical depth is close to the soil surface.

5. Conclusion

Based on the Laplace integral transformation and finite-difference method, approximate solution of permeability coefficient of unsaturated soil has been derived. Moreover, the stability and deformation characteristics of soldier piles are analyzed. The conclusions can be obtained as follows:

(1) In the process of rainfall infiltration, embedding stability of soldier piles declines obviously with rainfall intensity and saturated permeability coefficient of soil.

(2) There is hysteresis for displacement response of retaining piles with rainfall. The displacement of pile top increases gradually after rainfall; the lag time decreases with the increase of soil saturated permeability coefficient. The rise of groundwater level will lead to a significant increase of displacement and bending moment of pile, especially the rise of deep water level.

(3) The influence of rainfall on the supporting structure of foundation pit in low-suction or low-permeability soil is relatively limited in terms of the moisture absorption of homogeneous soil.

(4) The suction head distribution is taken as the initial condition for permeability coefficient calculation in the second stage. The errors are linearly distributed. The calculation results have high accuracy, which avoids the complexity caused by the initial condition in the form of series used in the analytical derivation.

Data Availability

The data used to support the findings of this study are included within the article. The readers can access the data through the figures within the article.

Conflicts of Interest

The authors declare that there are no conflicts of interest regarding the publication of this paper.

Acknowledgments

This research was funded by specialized research fund for the Doctoral Program of China (grant number 20120162110023).

References

[1] J.-M. Wu, G.-X. Li, and C.-H. Wang, "Effect of matric suction of unsaturated soil on the estimation of the load internal force on supporting structure for deep excavation," *Industrial Construction*, vol. 33, no. 7, pp. 6–10, 2003.

[2] U. A. Aqtash and P. Bandini, "Prediction of unsaturated shear strength of an adobe soil from the soil–water characteristic curve," *Construction & Building Materials*, vol. 98, pp. 892–899, 2015.

[3] E. A. Khaboushan, H. Emami, M. R. Mosaddeghi, and A. R. Astaraei, "Estimation of unsaturated shear strength parameters using easily-available soil properties," *Soil and Tillage Research*, vol. 184, pp. 118–127, 2018.

[4] E.-C. Leong and H. Abuel-Naga, "Contribution of osmotic suction to shear strength of unsaturated high plasticity silty soil," *Geomechanics for Energy and the Environment*, vol. 15, pp. 65–73, 2018.

[5] J. Kim, W. Hwang, and Y. Kim, "Effects of hysteresis on hydro-mechanical behavior of unsaturated soil," *Engineering Geology*, vol. 245, pp. 1–9, 2018.

[6] L.-Z. Wu and R.-Q. Huang, "Analytical analysis of coupled seepage in unsaturated soils considering varying surface flux," *Chinese Journal of Geotechnical Engineering*, vol. 33, no. 9, pp. 1370–1375, 2011.

[7] L. Z. Wu, L. M. Zhang, and X. Li, "One-dimensional coupled infiltration and deformation in unsaturated soils subjected to varying rainfall," *International Journal of Geomechanics*, vol. 16, no. 2, article 06015004, 2015.

[8] S. Oh and N. Lu, "Slope stability analysis under unsaturated conditions: case studies of rainfall-induced failure of cut slopes," *Engineering Geology*, vol. 184, pp. 96–103, 2015.

[9] H.-Q. Dou, T.-C. Han, X.-N. Gong, and J. Zhang, "Probabilistic slope stability analysis considering the variability of hydraulic conductivity under rainfall infiltration-redistribution conditions," *Engineering Geology*, vol. 183, pp. 1–13, 2014.

[10] Y.-S. Song, B.-G. Chae, and J. Lee, "A method for evaluating the stability of an unsaturated slope in natural terrain during rainfall," *Engineering Geology*, vol. 210, pp. 84–92, 2016.

[11] D.-M. Sun, X.-M. Li, P. Feng, and Y.-G. Zang, "Stability analysis of unsaturated soil slope during rainfall infiltration using coupled liquid-gas-solid three-phase model," *Water Science and Engineering*, vol. 9, no. 3, pp. 183–194, 2016.

[12] S. E. Cho, "Stability analysis of unsaturated soil slopes considering water-air flow caused by rainfall infiltration," *Engineering Geology*, vol. 211, pp. 184–197, 2016.

[13] T. L. T. Zhan and C. W. W. Ng, "Analytical analysis of rainfall infiltration mechanism in unsaturated soils," *International Journal of Geomechanics*, vol. 4, no. 4, pp. 273–284, 2004.

[14] T. L. T. Zhan, G. W. Jia, Y.-M. Chen, D. G. Fredlund, and H. Li, "An analytical solution for rainfall infiltration into an unsaturated infinite slope and its application to slope stability analysis," *International Journal for Numerical and Analytical Methods in Geomechanics*, vol. 37, no. 12, pp. 1737–1760, 2013.

[15] C. W. W. Ng, L. T. Zhan, C. G. Bao, D. G. Fredlund, and B. W. Gong, "Performance of an unsaturated expansive soil slope subjected to artificial rainfall infiltration," *Géotechnique*, vol. 53, no. 2, pp. 143–157, 2003.

[16] N. Lu and J. Godt, "Infinite slope stability under steady unsaturated seepage conditions," *Water Resources Research*, vol. 44, no. 11, pp. 1–13, 2008.

[17] C.-H. Zhang, Q.-H. Zhang, and J.-H. Zhao, "Developments for unified solution of shear strength and ultimate bearing capacity of foundation in unsaturated soils," *Rock and Soil Mechanics*, vol. 31, no. 6, pp. 1871–1876, 2010.

[18] N. Lu and W. J. Likos, *Unsaturated Soil Mechanics*, Wiley, Hoboken, NJ, USA, 2004.

[19] W. R. Gardner, "Some steady-state solutions of the unsaturated moisture flow equation with application to evaporation from a water table," *Soil Science*, vol. 85, no. 4, pp. 228–232, 1958.

[20] R. Srivastava and T.-C. J. Yeh, "Analytical solutions for one-dimensional, transient infiltration toward the water table in homogeneous and layered soils," *Water Resources Research*, vol. 27, no. 5, pp. 753–762, 1991.

[21] N. Li and J.-C. Xu, "Simulation of Deformation of infinite soil slope," *Chinese Journal of Geotechnical Engineering*, vol. 34, no. 12, pp. 2325–2330, 2012.

[22] M. T. van Genuchten, "A closed-form equation for predicting the hydraulic conductivity of unsaturated Soils1," *Soil Science Society of America Journal*, vol. 44, no. 5, pp. 892–898, 1980.

[23] L.-J. Chen, Y.-J. Sun, and Z.-G. Wang, "Research of finite difference method on retaining structures with internal braces in deep excavation engineering," *Chinese Journal of Rock Mechanics and Engineering*, vol. 35, no. 1, pp. 3316–3322, 2016.